Article

A Quantum Dynamical Treatment of Symmetry-Induced Kinetic Isotope Effects in the Formation of He

Junkai Xie, Bill Poirier, and Gregory I. Gellene

J. Am. Chem. Soc., **2005**, 127 (48), 16969-16975• DOI: 10.1021/ja0517419 • Publication Date (Web): 11 November 2005

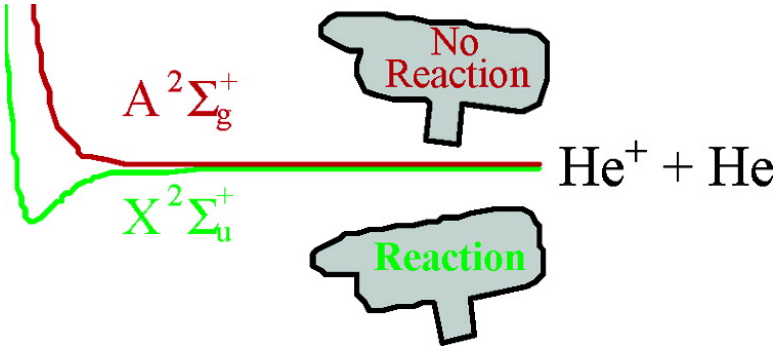

More About This Article

Additional resources and features associated with this article are available within the HTML version:

- Supporting Information
- Links to the 1 articles that cite this article, as of the time of this article download
- Access to high resolution figures
- Links to articles and content related to this article
- Copyright permission to reproduce figures and/or text from this article

View the Full Text HTML

J|A|C|S
ARTICLES
Published on Web 11/11/2005

A Quantum Dynamical Treatment of Symmetry-Induced Kinetic Isotope Effects in the Formation of He_2^+

Junkai Xie, Bill Poirier, and Gregory I. Gellene*

Contribution from the Department of Chemistry and Biochemistry, Texas Tech University, Lubbock, Texas 70409-1061

Received March 18, 2005; E-mail: greg.gellene@ttu.edu

Abstract: Kinetic isotope effects for He_2^+ formation are calculated quantum dynamically using high-quality Born−Oppenheimer (BO) potentials for two electronic states of He_2^+ and an accurate treatment of all nonadiabatic BO corrections. The two potentials are coupled only when the helium isotopes are different, and the calculations reveal that this coupling is sufficient to allow the two sets of distinguishable reactants, $^4He^+ + {}^3He$ or $^3He^+ + {}^4He$, to yield He_2^+ with comparable efficiency over a wide temperature range. Consequently, the potential coupling provides a significant formation rate enhancement for the low isotopic symmetry reactants, as compared to the symmetrical cases (e.g., $^4He^+ + {}^4He$ or $^3He^+ + {}^3He$). The computed symmetry-induced kinetic isotope effects (SIKIEs) are in substantial agreement with the available experimental results and represent the first theoretical demonstration of this unusual kinetic phenomenon. Possible application of SIKIE to ozone formation and other chemical systems is discussed.

Introduction

In dynamical treatments of chemical reactions involving asymptotically degenerate or near-degenerate Born−Oppenheimer (BO) potential energy surfaces (PESs), where detailed information about possible coupling between the PESs is unavailable, it is common to assume that the probability of accessing a particular surface of electronic degeneracy, g_e, is well approximated by the transition state theory based statistical weighting factor, $g_e/Q_{elec}^{react}(T)$, where $Q_{elec}^{react}(T)$ is the electronic partition function of the reactants.[1] However, for at least as long as this approach has been followed, it has been known that nonadiabatic coupling between PESs can lead to a breakdown of the BO approximation that can allow essentially *all* reactant collisions to access the particular PES responsible for the chemical reaction of interest.[2] If these BO breakdowns have a substantial isotope dependence, it is possible that unexpected kinetic isotope effects (KIEs) (i.e., those not directly due to the different isotopic masses) may occur. In particular, for chemistry involving small molecules, nuclear permutation symmetry considerations may prohibit, or at least greatly restrict, the relevant nonadiabatic coupling when the reactants contain identical isotopes. These couplings would then be "turned on" only when the isotopes are distinguishable, allowing such reactants to more effectively access the relevant PES, and thus give rise to a symmetry-induced KIE (SIKIE). More specifically, we denote this situation as a "type 2 SIKIE" because at least two BO PESs are involved.

In 1987, the ratio of product O_2 molecules in the $^1\Delta_g$ versus the $^3\Sigma_g^-$ electronic states, following photoexcitation of ozone in the Chappuis band, was found to depend on the isotopic symmetry of the O_2,[3] making this an example of a type 2 SIKIE in a "half collision" context. Between 1992 and 1996, a series of experimental ion−molecule reaction studies provided strong evidence for type 2 SIKIE in the "full collision" context, occurring in the three-body formation of O_4^+,[4] He_2^+,[5] $CO_2^+(CO_2)$,[6] and $CO_2^+(Ar)$.[7] The results were interpreted within the framework of a general symmetry correlation scheme[8] as applied to the first collision of the two-step energy transfer mechanism for three-body association. In this mechanism, two reactants first collide to form an intermediate metastable form of the association product known as an "energized complex", which is then stabilized by energy transfer in subsequent collisions. Although this approach provided a context for understanding the observed type 2 SIKIE in a general way, no detailed dynamical calculations that could be compared to experimental results were performed.

In some of the ion−molecule reaction studies,[5,6] a type 1 SIKIE was also identified, so-named because only one PES need be involved. The type 1 effect was proposed to be operating in the energy transfer collision of the two-step association mechanism and has its origin in the well-understood effects of nuclear permutation symmetry on the density of states (i.e., a symmetric isotopologue will have a lower density of states than its asymmetric counterparts). Very recently, direct theoretical support for this energy transfer kind of type 1 SIKIE has been provided by a quantum dynamical study of KIEs in the association reaction, $2Ne + H \rightarrow Ne_2 + H$.[9] An additional symmetry-dependent, density-of-states issue has been raised recently by Marcus et al.[10−13] in the context of ozone formation,

(1) Truhlar, D. G. *J. Chem. Phys.* **1972**, *56*, 3189.
(2) Muckerman J. T.; Newton, M. D. *J. Chem. Phys.* **1972**, *56*, 3191.
(3) Levene, H. B.; Nieh, J.-C.; Valentini, J. J. *J. Chem. Phys.* **1987**, *87*, 2583.
(4) Griffith, K. S.; Gellene, G. I. *J. Chem. Phys.* **1992**, *96*, 4403.
(5) Gellene, G. I. *J. Phys. Chem.* **1993**, *97*, 34.
(6) Yoo, R. K.; Gellene, G. I. *J. Chem. Phys.* **1995**, *102*, 3227.
(7) Yoo, R. K.; Gellene, G. I. *J. Chem. Phys.* **1996**, *105*, 177.
(8) Gellene, G. I. *J. Chem. Phys.* **1992**, *96*, 4387.
(9) Pack, R. T.; Walker, R. B. *J. Chem. Phys.* **2004**, *121*, 800.

where the absence of kinetic and potential coupling terms in the symmetric isotopologue appears to limit the available phase-space, thus inhibiting association. Most recently, this idea has been extended to explain "mass-independent" oxygen isotope effects in some of the oldest known solids in the solar system, namely, the calcium−aluminum-rich inclusions in chondritic meteorites.[15]

Although currently, experimental evidence for type 2 SIKIE is available only in the context of termolecular association and photoinduced dissociation, in principle, there is no reason the effect could not occur in a bimolecular reaction involving atomic rearrangement as reactants are transformed into products. In fact, it has been speculated[16] that the $H_2^+ + H_2 \rightarrow H_3^+ + H$ proton/atom transfer reaction may exhibit type 2 SIKIE at low temperature, where conservation of energy considerations would limit exchange between angular momentum arising from H_2^+/H_2 orbital motion and individual molecular rotation. In addition, there are a large number of so-called "mass-independent" isotope effects that have been reported in the literature,[17,18] many of which may have nuclear permutation symmetry-based explanations.

The purpose of the present study is to build on the symmetry-based correlation scheme used previously to rationalize type 2 SIKIE[8] and to place the phenomenon on a solid theoretical basis, through a detailed quantum dynamical study of the initial association step of the two-step energy transfer mechanism for He_2^+ formation:

$$^{a}He^+ + {}^{b}He \rightleftarrows (^{a}He^{b}He^+)^* \quad (1)$$

$$(^{a}He^{b}He^+)^* + {}^{c}He \rightarrow He_2^+ + He \quad (2)$$

In reactions 1 and 2, superscripts denote the particular isotope of helium (3 or 4), and $(He_2^+)^*$ denotes the energized complex form of the associated product. In the first step (reaction 1), an ion and a neutral atom collide to form the metastable energized complex. In the second step (reaction 2), the complex collides inelastically with a third atom, ^{c}He, resulting in a transfer of energy that stabilizes the associated product, He_2^+.

The physics of the low-energy electronic states of He_2^+ bears a strong analogy to those of H_2^+, the simplest molecule, which has been extensively studied[19−22] experimentally and theoretically. Both systems have deeply bound ground states and weakly bound first excited states that are asymptotically degenerate for symmetric isotopologues and nondegenerate for asymmetric isotopologues. Furthermore, in both cases, these two electronic states are sufficiently energetically isolated from all other excited BO states that only the two states need to be considered for an accurate description of the low-energy bound and resonance states. However, the two systems differ in at least one technical and one practical aspect. Technically, He_2^+ has three electrons, whereas H_2^+ has only one, so that multielectron interaction effects must be considered in the theoretical consideration of He_2^+, which, of course, are absent for H_2^+. Practically, three-body association reactions forming He_2^+ have been extensively studied (ref 23 and references therein), whereas chemistry analogous to reactions 1 and 2 that leads to H_2^+ formation (e.g., $H^+ + H + M \rightarrow H_2^+ + M$) has yet to be considered in detail. Although the strong analogy between the physics of the first two electronic states of He_2^+ and H_2^+ suggests that the three-body formation of H_2^+ would demonstrate type 2 SIKIE, we are unaware of any experimental or theoretical treatment of this issue.

A very recent quantum dynamical study of He_2^+ formation[23] has demonstrated the validity of reactions 1 and 2 for describing the dominant reaction mechanism under the conditions generally used in the experimental studies[5] and, thus, establishes the two-step energy transfer mechanism as the appropriate framework for the present consideration of isotope effects. Although the primary focus is the effect of type 2 SIKIE on reaction 1, the usual mass-dependent KIEs also operating in reaction 1 will be considered as a matter of course. An exact determination of all KIEs for this system would require consideration of the full He_3^+ PES[24] (possibly, more than one) in order to properly treat reaction 2. This is beyond the scope of the present study; however, we do treat reaction 2 in an approximate manner, for which the isotopic identity of the final products can be specified under various limiting assumptions, providing predictions that can be compared to the experimental results. Despite the approximate treatment of reaction 2, the present approach is sufficient to provide the first fully theoretical demonstration of type 2 SIKIE.

Theoretical Methods

Kinetic Model. Following ref 25, the three-body recombination rate for the two-step mechanism can be expressed as

$$k_r(T) = (1 + \delta_{bc})Q_{ab}(T)^{-1}\sum_i e^{-\beta E_i}k_i\omega_i/(k_i + \omega_i) \quad (3)$$

where $k_r(T)$ is a second-order effective thermal rate constant, and the summation is over all of the metastable resonance states associated with the energized complex, $(He_2^+)^*$. The quantities E_i, k_i, and ω_i are, respectively, the energy, the unimolecular decay rate constant, and the stabilization collision frequency for the ith resonance state of $(He_2^+)^*$. The quantity $Q_{ab}(T)$ is the reactant ($^{a}He^+ + {}^{b}He$ relative motion) partition function per unit volume, and $\beta = k_BT$, where k_B is Boltzmann's constant. The factor $(1 + \delta_{bc})$ is required to account for a factor of 2 which arises from the dual role of He as both reactant and third body, and the inability of quantum mechanics to distinguish which is which when ^{b}He and ^{c}He are identical isotopes.

For reaction 2, which involves a molecular ion and a nonpolar neutral atom, the collision rate can be ordinarily well estimated by the ion-induced dipole-based Langevin expression.[26]

$$k_L = (4\pi^2\alpha q^2/\mu_{ab,c})^{1/2} \quad (4)$$

where α is the polarizability of He [1.3793 au (atomic units)], q is the

(10) Hathorn, B. C.; Marcus, R. A. *J. Chem. Phys.* **1999**, *111*, 4087.
(11) Hathorn, B. C.; Marcus, R. A. *J. Chem. Phys.* **2000**, *113*, 9497.
(12) Gao, Y. Q.; Marcus, R. A. *Science* **2001**, *293*, 259.
(13) Gao, Y. Q.; Marcus, R. A. *J. Chem. Phys.* **2002**, *116*, 137.
(14) Gao, Y. Q.; Chen, W. C.; Marcus, R. A. *J. Chem. Phys.* **2002**, *117*, 1536.
(15) Marcus, R. A. *J. Chem. Phys.* **2004**, *121*, 8201.
(16) Picconatto, C. A.; Gellene, G. I. *J. Phys. Chem.* **1993**, *97*, 13629.
(17) Weston, R. E. *Chem. Rev.* **1999**, *99*, 2115.
(18) Brenninkmeijer, C. A. M.; Janssen, C.; Kaiser, J.; Röckmann, T.; Rhee, T. S.; Assonov, S. S. *Chem. Rev.* **2003**, *103*, 5125.
(19) Carrington, A.; Leach, C. A.; Marr, A. J.; Moss, R. E.; Pyne, C. H.; Steimle, T. C. *J. Chem. Phys.* **1993**, *98*, 5290.
(20) Orlikowski, T. *Mol. Phys.* **1994**, *81*, 667.
(21) Leach, C. A.; Moss, R. E. *Annu. Rev. Phys. Chem.* **1995**, *46*, 55.
(22) Wells, E.; Esry, B. D.; Carnes, K. D.; Ben-Itzhak, I. *Phys. Rev. A* **2000**, *62*, Art. No. 062707.
(23) Xie, J.; Poirier, B.; Gellene, G. I. *J. Chem. Phys.* **2003**, *119*, 10678.
(24) Chang, D. T.; Gellene, G. I. *J. Chem. Phys.* **2003**, *119*, 4694.
(25) Miller, W. H. *J. Phys. Chem.* **1995**, *99*, 12387.
(26) Steinfeld, J. I.; Francisco, J. S.; Hase, W. L. *Chemical Kinetics and Dynamics*; Prentice Hall: Englewood Cliffs, New Jersey, 1989.

ionic charge (+1 au), and $\mu_{ab,c}$ is the ($^aHe^bHe^+$)*−^cHe reduced mass [atomic mass of ^3He and ^4He are 3.01602931 and 4.002603250 amu (atomic mass units), respectively[27]].

In terms of k_L, ω_i can be written as

$$\omega_i = \beta_{L_i} k_L \rho_{^cHe} \tag{5}$$

where $\rho_{^cHe}$ is the number density of ^cHe, and β_{L_i} is the efficiency with which the third-body collision actually induces stabilization of the associated product from the *i*th resonance state. As discussed previously, absent a careful dynamical analysis of reaction 2, detailed information on β_{L_i} is unavailable. As the present focus is on type 2 SIKIEs in reaction 1, we assume a uniform stabilization efficiency, that is, we take $\beta_{L_i} = \beta_L$ for all resonance states. Although this may appear to be a questionable assumption, a previous study[23] justified this approach for a particular isotopologue, noting that the resonance states that contribute significantly to the dimer formation rate have stabilization pathways involving similar angular momentum (ΔN) and energy (ΔE) changes. That work found that $\beta_L = 0.65$ gave excellent agreement with the experimental He_2^+ association rate over the temperature range of 30−350 K, under conditions where only ^4He was present (i.e., no consideration of isotope effects). However, even under a uniform stabilization efficiency assumption, β_L could be expected to depend on isotopic composition because of the resulting changes in the ΔN and ΔE characteristics of the important stabilization pathways. Nevertheless, absent any information on the isotopic dependence of β_L, the value of 0.65 will be used throughout. Although this approach may suffer in terms of quantitative comparisons with experimental results, it has the advantage that the predicted isotope effects are independent of the particular value assigned to β_L.

Finally, a third-order effective thermal rate constant that can be compared to experiment is obtained via

$$k_{eff}^{abc}(T) = k_r(T)/\rho_{^cHe} = k_r(T)\beta_L k_L/\omega \tag{6}$$

where the superscripts on k_{eff} denote the isotopic identity of the ion (a) and the neutral (b) that comprise the energized complex, as well as the third-body (c). Often, the unimolecular decay rate constants of the resonance states span a very broad range encompassing orders of magnitude. If the total number of resonance states within the relevant energy range is not too large, the likelihood of there being a k_i in the vicinity of ω is very small. Under these conditions (appropriate to the present study), the functional dependence of k_{eff} can be made more clear by noting that only resonance states for which $k_i \gg \omega$ will appreciably contribute to He_2^+ association. Ignoring the other resonance states, and considering the low-pressure limit (appropriate to the conditions of our study), the expression for $k_{eff}^{abc}(T)$ becomes

$$k_{eff}^{abc}(T) \approx (1+\delta_{bc})Q_{ab}(T)^{-1}\beta_L k_L \sum_i e^{-\beta E_i} \tag{7}$$

which is independent of $\rho_{^cHe}$. However, eq 7 is presented for illustrative purposes only, and all reported values of $k_{eff}^{abc}(T)$ are calculated using eq 6. Equation 7 also makes it clear (as does eq 6) that ratios of $k_{eff}^{abc}(T)$ will be independent of the particular β_L value used. Finally, we note that conventional mass-dependent KIEs enter eq 7 through the mass dependence of $Q_{ab}(T)$ and k_L, whereas type 2 SIKIEs arise from the consequence of symmetry on the energy distribution and other properties of the resonance states.

Resonance State Calculations. The investigation of type 2 SIKIE requires the consideration of multiple electronic states and the interaction among them. Specifically for reaction 1, the deeply bound ($D_e \sim 20\,000\ cm^{-1}$) ground $X^2\Sigma_u^+$ and largely repulsive ($D_e \sim 17\ cm^{-1}$) first excited $A^2\Sigma_g^+$ BO PESs of He_2^+ are relevant (Figure 1). The electronic wave functions associated with these PESs will be denoted as $\Phi_e^n(r;R)$, where r and R represent the electron coordinates and nuclear separation, respectively, and the index n varies over the values u and g denoting the $X^2\Sigma_u^+$ and $A^2\Sigma_g^+$ states, respectively. These electronic states are asymptotically degenerate in the adiabatic (i.e., noninteracting BO PES with or without first-order diagonal corrections) approximation and remain degenerate for identical isotopes because the nonadiabatic coupling between the states vanishes in this case. They become asymptotically nondegenerate in the diabatic representation only for asymmetric isotopologues, when nonadiabatic interactions are included (the resultant $^3He^+ + {}^4He$ state is energetically lower than the $^4He^+ + {}^3He$ state).

If electron spin interactions (expected to be small for energetically isolated Σ states) and nuclear hyperfine interactions (generally small and identically zero for ^4He) are neglected for He_2^+, a complete, compact 2×2 matrix representation for the nuclear motion Hamiltonian for the two electronic state coupled system can be written as:[28]

$$\hat{\boldsymbol{H}} = \left[\left(\frac{-\hbar^2}{2\mu_{a,b}}\right)\frac{d^2}{dR^2} + \frac{N(N+1)\hbar^2}{2\mu_{a,b}R^2}\right]\boldsymbol{I} + \epsilon(R) + \boldsymbol{w}_1(R)\frac{d}{dR} \tag{8}$$

where $\mu_{a,b}$ is the reduced mass of the reaction 1 reactants; N is the Hund's case (b) angular momentum quantum number, $\boldsymbol{I}$ is the two-dimensional identity matrix, and $\boldsymbol{w}_1(R)$ is the nonadiabatic matrix arising from the action of the first derivative with respect to R operating on the electronic states with matrix elements given by

$$w_1^{nm}(R) = -\frac{\hbar^2}{\mu_{a,b}}\left\langle \Phi_e^n(r;R)\left|\frac{\partial}{\partial R}\right|\Phi_e^m(r;R)\right\rangle \tag{9}$$

In eq 8 above, the quantity $\epsilon(R)$ is the nonadiabatic effective potential matrix given by

$$\epsilon(R) = \boldsymbol{w}_{mp}(R) + \boldsymbol{w}_l(R) + \boldsymbol{w}_2(R) + \boldsymbol{V}_e(R) \tag{10}$$

where $\boldsymbol{V}_e(R)$ is the adiabatic potential matrix (i.e., a diagonal matrix containing the $X^2\Sigma_u^+$ and $A^2\Sigma_g^+$ BO PESs) and $\boldsymbol{w}_{mp}(R)$, $\boldsymbol{w}_l(R)$, and $\boldsymbol{w}_2(R)$ represent the nonadiabatic corrections arising, respectively, from the mass polarization operator, the electron angular momentum operator ($\hat{\boldsymbol{L}}$) with respect to the center of nuclear mass, and the second derivative with respect to R operating on the electronic states, with the individual matrix elements given by

$$w_{mp}^{nm}(R) = -\frac{\hbar^2}{2M}\langle \Phi_e^n(r;R)|\sum_{i,j=1}^{3}\nabla_i\cdot\nabla_j|\Phi_e^m(r;R)\rangle \tag{11}$$

$$w_l^{nm}(R) = \frac{1}{2\mu R^2}\langle \Phi_e^n(r;R)|\hat{L}^2|\Phi_e^m(r;R)\rangle \tag{12}$$

$$w_2^{nm}(R) = -\frac{\hbar^2}{2\mu}\left\langle \Phi_e^n(r;R)\left|\frac{\partial^2}{\partial R^2}\right|\Phi_e^m(r;R)\right\rangle \tag{13}$$

In eq 11, M is the total nuclear mass, and the subscripts i and j refer to electrons.

All the R-dependent quantities in eqs 8 and 10 have been calculated previously and accurately fit to analytical functions over the relevant range of R (1.2−100 au).[29] These functions have also been used previously to provide the most accurate representation currently available, for both the low and high ro-vibrational levels of the ground and the bound levels of the excited electronic states, indicating that they should be of sufficient quality for the present dynamical study.

The two BO PESs are coupled only for asymmetric isotopologues and then only through $\boldsymbol{w}_1$, $\boldsymbol{w}_2$, and $\boldsymbol{w}_l$, which are the only nondiagonal matrices in eqs 8 and 10. The magnitude of the off-diagonal elements

(27) Audi, G; Wapstra, A. H. *Nucl. Phys. A* **1993**, *566*, 1.

(28) Kupperman A.; Abrol, R. *Adv. Chem. Phys.* **2002**, *124*, 283.
(29) Xie, J.; Poirier, B.; Gellene, G. I.; *J. Chem. Phys.* **2005**, *122*, 184310.

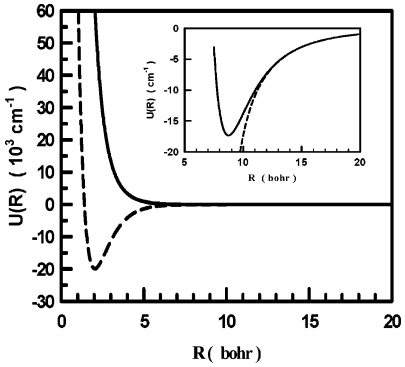

Figure 1. Plot of the Born−Oppenheimer potentials for the ground $X^2\Sigma_u^+$ and first excited $A^2\Sigma_g^+$ electronic states of He_2^+ as determined in ref 26. The inset plot shows the shallow well present in the $A^2\Sigma_g^+$ potential.

from the $\boldsymbol{w}_1$ term is about 10−100 times smaller than those of either $\boldsymbol{w}_2$ or $\boldsymbol{w}_l$, which for this system are found to have typical values of a few cm^{-1}. Setting $\boldsymbol{w}_{mp}(R) = \boldsymbol{w}_l(R) = \boldsymbol{w}_1(R) = \boldsymbol{w}_2(R) = 0$ (where 0 is the two-dimensional null matrix) recovers the BO approximation. The resulting uncoupled Schrödinger equations were solved for $N = 0$ using a sinc function discrete variable representation (DVR).[30] These solutions, in turn, were used to develop a potential optimized DVR basis,[31] which was then employed to solve the coupled, nonadiabatic Schrödinger equations for arbitrary N.

The required unimolecular decay rate, k_i, associated with the ith resonance state is just the inverse of the lifetime (i.e., $k_i = \Gamma_i/\hbar$, where Γ_i is the resonance width). Complex absorbing potential (CAP) techniques[32] are very convenient in this regard in that they enable one to compute the resonance widths directly, that is, without the need for Lorentzian fitting, etc. In this approach, an optimized polynomial CAP, $-iW(R)$, is added to the diagonal components of $\boldsymbol{V}_e(R)$ in the asymptotic large R region to absorb outgoing flux (an identical CAP was used for both BO PESs). This has the effect of converting the Hamiltonian operator into a non-Hermitian, but complex symmetric, effective Hamiltonian, $\hat{\boldsymbol{H}}' = \hat{\boldsymbol{H}} - [iW(R)]\boldsymbol{I}$, which has complex eigenvalues ($E_i - i\Gamma_i/2$). Before solving the Schrödinger equation with $\hat{\boldsymbol{H}}'$, an adiabatic-to-diabatic (ATD) transformation[28] was performed. This is a standard, R-dependent 2 × 2 matrix transformation that is applied to $\hat{\boldsymbol{H}}'$ to minimize the impact of the $\boldsymbol{w}_1(R)\ d/dR$ term, which would otherwise be difficult to deal with numerically.

The transformed $\hat{\boldsymbol{H}}'$ problem was solved repeatedly for all relevant values of N. In each case, all relevant resonances were computed, and the resultant E_i and Γ_i values were incorporated into the sum in eq 3, with the appropriate $(2N + 1)$ weighting factor due to the azimuthal degeneracy of the rotational states. An additional weighting factor arises from a consideration of nuclear spin (NS) statistics. Because the two electronic states are not coupled for identical isotope collisions and because the uncoupled excited electronic state does not support any resonance states, only NS statistics appropriate to the ground electronic state symmetry are required for the symmetric isotopologues. Specifically, a NS weighting of 0 and 1 is applied to the even and odd values of N, respectively, for $^4He^+ + {}^4He$ (nuclear spin equals 0), whereas a NS weighting of 3/4 and 1/4 is applied to even and odd values of N, respectively, for $^3He^+ + {}^3He$ (nuclear spin equals $\hbar/2$). For $^3He^+ + {}^4He$ and $^4He^+ + {}^3He$ collisions, a NS weighting of 1 is appropriate for all values of N.

Results

Computed values for $k_{eff}^{33c}(T)$ and $k_{eff}^{44c}(T)$ (i.e., initial collisions of identical isotopes) and $k_{eff}^{34c}(T)$ and $k_{eff}^{43c}(T)$ (i.e., initial collisions of distinguishable isotopes) over the temperature range of 1−400 K are shown in Figure 2a and b, respectively. The $k_{eff}^{444}(T)$ curve is almost identical to that reported previously[23] because the addition of the small diagonal nonadiabatic terms to the potential has only very minor effects on the properties of the resonance states, and these small differences are essentially washed out by the thermal averaging. Each of the curves shows a negative temperature dependence over most of the temperature range investigated, with a rate maximum occurring at low temperature. This maximum is particularly large and sharp for $k_{eff}^{34c}(T)$. In general, the reaction rates for identical reactants (Figure 2a) are smaller than those for the isotopically asymmetric case (Figure 2b). In each plot, the four curves organize themselves naturally into two groups: $k_{eff}^{334}(T) \approx k_{eff}^{443}(T)$ and $k_{eff}^{333}(T) \approx k_{eff}^{444}(T)$ in Figure 2a, and $k_{eff}^{343}(T) \approx k_{eff}^{434}(T)$ and $k_{eff}^{344}(T) \approx k_{eff}^{433}(T)$ in Figure 2b, with each pair differing by about a factor of 2 from the other pair within the same plot. This factor of 2 results largely from the $(1 + \delta_{bc})$ factor in eq 7. It might be expected that the ratios $k_{eff}^{333}(T)/k_{eff}^{334}(T)$, $k_{eff}^{444}(T)/k_{eff}^{443}(T)$, $k_{eff}^{344}(T)/k_{eff}^{343}(T)$, and $k_{eff}^{433}(T)/k_{eff}^{434}(T)$ would be exactly 2 because the partition function factor and the sum in eq 7 exactly cancel in each ratio. However, the contribution of $\mu_{ab,c}$ via k_L modifies these ratios by about 10% (specifically, by a factor of about 1.094, 0.906, 0.910, and 1.099, respectively).

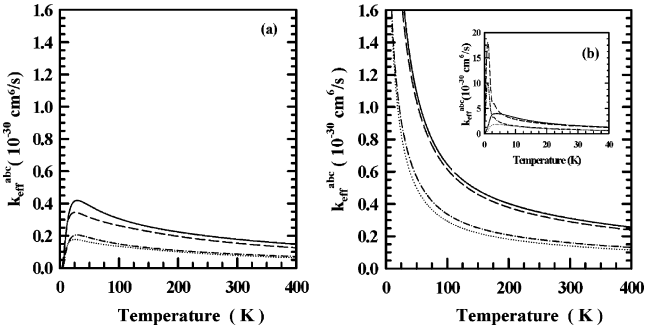

Figure 2. Plot of calculated values of $k_{eff}^{abc}(T)$ after eq 6 for initial collisions of (a) identical and (b) distinguishable helium isotopes. In (a), abc = 333, 444, 334, and 443 are represented, respectively, by solid, dashed, dot−dashed, and dotted curves. In (b), abc = 433, 344, 343, and 434 are represented, respectively, by solid, dashed, dot−dashed, and dotted curves. The inset in (b) emphasizes the low-temperature behavior of distinguishable isotope formation rate constants.

Discussion

Effective Rate Constants. As pointed out in the previous study,[23] the negative temperature dependence observed for all the rate constant curves arises from the sum of the Boltzmann terms in eq 7 for the resonance states making up an increasing fraction of the partition function as the temperature decreases. This leads to an expected rate constant maximum near $\beta E_{low} \approx 3/2$, where E_{low} is the lowest energy resonance for which $k_{low} \gg \omega$. The maxima in these curves occur at similar temperatures for $k_{eff}^{33c}(T)$ and $k_{eff}^{44c}(T)$ because E_{low} is comparable in these cases (15.87 cm^{-1}, $N = 6$ and 17.19 cm^{-1}, $N = 9$, respectively). The corresponding maxima for $k_{eff}^{43c}(T)$ (Figure 2b, inset) are higher and occur at lower temperature than those of either $k_{eff}^{33c}(T)$ or $k_{eff}^{44c}(T)$ because, in the former case, E_{low} is only 2.51 cm^{-1} ($N = 7$) with respect to the asymptotic energy of the upper ($^4He^+ + {}^3He$) diabatic PES. The wave function for this resonance is depicted in Figure 3, and an examination of its properties yields substantial insight into the dynamical conse-

(30) Colbert D. T.; Miller, W. H. *J. Chem. Phys.* **1992**, *96*, 1982.
(31) Light, J. C.; Carrington, T., Jr. *Adv. Chem. Phys.* **2000**, *114*, 263.
(32) Muga, J. G.; Palao, J. P.; Navarro, B.; Egusquiza, I. L. *Phys. Rep.* **2004**, *395*, 357.

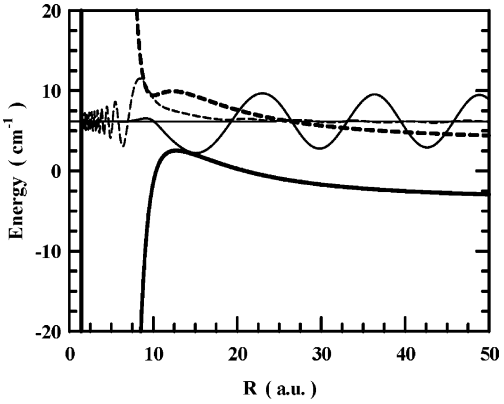

Figure 3. Plot of the $N = 7$ diabatic effective potentials for the ground (bold, solid curve) and first excited (bold, dashed curve) electronic states of $(^4He^3He)^+$. Also depicted is the projection of the shape resonance state wave function supported by these potentials onto the ground (thin, solid curve) and excited (thin, dashed curve) electronic states. Although the amplitude of the two wave functions is plotted on the same scale, that scale is arbitrary with respect to the energy axis labels. The horizontal line indicates the resonance state energy.

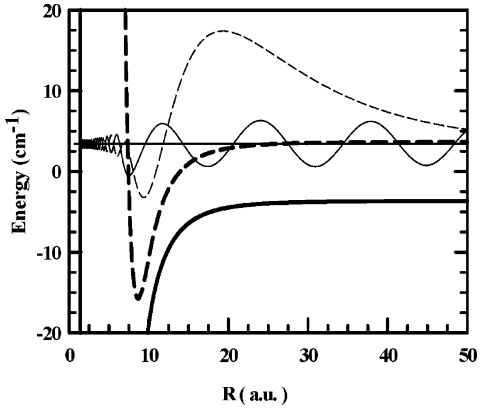

Figure 4. Plot of the $N = 0$ diabatic effective potentials for the ground (bold, solid curve) and first excited (bold, dashed curve) electronic states of $(^4He^3He)^+$. Also depicted is the projection of the Feshbach resonance state wave function supported by these potentials onto the ground (thin, solid curve) and excited (thin, dashed curve) electronic states. Although the amplitude of the two wave functions is plotted on the same scale, that scale is arbitrary with respect to the energy axis labels. The $v = 1$ character of the excited state projection of the resonance is apparent from the nodal structure in the well region of excited potential. The horizontal line indicates the resonance state energy.

quences of removing nuclear symmetry. The "shape resonance" character (so-named because the resonance is induced by the shape of the PES) arises entirely from the lower ($^3He^+ + {}^4He$) diabatic PES, where the resonance state energy lies about 3.61 cm^{-1} above the angular momentum barrier in the effective diabatic potential. Even though the upper diabatic PES does not, by itself, support a shape resonance, $N = 7$ collisions beginning on the upper diabatic PES with a translational energy of about 2.51 cm^{-1} will, through inter-PES coupling, access the lower diabatic PES shape resonance, just as an $N = 7$ collision beginning on the lower diabatic PES with a translational energy of about 9.71 cm^{-1} does. Indeed, this resonance would be expected to dominate in the electron transfer process

$$^3He^+ + {}^4He \rightleftarrows {}^4He^+ + {}^3He \qquad (14)$$

for low-energy collisions of $N = 7$ reactants and products, and a quantum dynamical study of reaction 14 is currently underway.

The above analysis clearly shows that the inter-PES coupling is sufficient to allow access to the lower diabatic PES resonance for reactants that begin the collision on *either* PES asymptote. Consequently, the three-body association reaction beginning with either $^3He^+ + {}^4He$ or $^4He^+ + {}^3He$ is expected to have a substantial kinetic advantage over reactions beginning with either $^3He^+ + {}^3He$ or $^4He^+ + {}^4He$. This enhancement factor, which is the essence of the type 2 SIKIE phenomena, has a completely different origin than, and operates in addition to, the expected approximate factor of 2 arising from nuclear spin statistics considerations. Thus, the often recommended procedure for treating a collision occurring on BO PESs with a 2-fold asymptotic degeneracy by the application of an ad hoc kinetic factor of 1/2, with the idea that only one surface leads to the reaction of interest, is clearly invalid in this case.

Finally, the maxima for $k_{\mathrm{eff}}^{34c}(T)$ (Figure 2b, inset) are larger, more peaked, and occur at lower temperatures than any of the others. These characteristics are the result of an extremely small E_{low} (0.046 or -7.284 cm^{-1}, with respect to $^3He^+ + {}^4He$ or $^4He^+ + {}^3He$, respectively), corresponding to a fundamentally different kind of resonance known as a "Feshbach resonance", as illustrated in Figure 4. In the present context, a Feshbach resonance occurs when a bound ro-vibrational state on the upper diabatic PES is able to dissociate on the lower diabatic PES, via inter-PES coupling. Note that unlike shape resonances, Feshbach resonances require multiple, coupled PESs and, therefore, only manifest in this system for asymmetric isotopologues. Note also that they can only be found at energies between the asymptotic values for the upper and lower PESs (i.e., at very low energies) and only for collisions of $^3He^+ + {}^4He$. For the present system, the lowest energy Feshbach resonance corresponds to the $(v, N) = (0, 1)$ ro-vibrational level of the upper diabatic potential. In fact, with the exception of the $(v, N) = (0, 0)$ level, the additional states that would otherwise be bound levels on the upper diabatic potential are actually Feshbach resonances for distinguishable isotopes. As such, to the extent that these resonances contribute to the overall reaction rate, they represent a mode of type 2 SIKIE not previously considered.

Product Ratios. Although product ratios of He_2^+ isotopic variants cannot be determined with certainty without detailed information about reaction 2, it is nevertheless instructive to consider these ratios under particular limiting dynamical assumptions. One such assumption is that no atom exchange takes place, so that the molecular product of reaction 2 is exclusively $^aHe^bHe^+$. Although at first consideration this may seem like an unrealistic assumption, it is supported by experimental studies of He_2^+ formation[5] and indirectly by theoretical studies of Ne_2 formation,[9] where the stabilization step was found to be dominated by Ne_2^* rotational state changes induced by relatively long-range angular momentum exchange between the Ne_2^* rotational angular momentum and the Ne_2^*/H orbital angular momentum. Although exchange is not possible in the 2Ne + H system (NeH has no bound levels in the ground electronic state), the long-range nature of the stabilization step (as opposed to the short-range nature of a vibration to translation energy transfer) would tend to inhibit atom exchange were it possible. Furthermore, the no exchange assumption allows the isotope effects of reaction 1 to be largely isolated and emphasized.

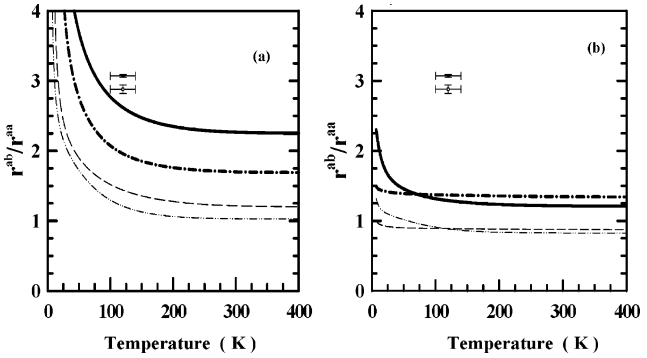

Figure 5. Comparison of asymmetric (r^{ab}) to symmetric (r^{aa}) He_2^+ isotopomer formation rate ratios calculated under the assumption for the energy transfer, stabilization step (reaction 2) of (a) no atom exchange, using eqs 15−17, and (b) statistical atom exchange, using eqs 19−21. In both (a) and (b), bold curves denote the use of the two PESs including coupling, thin curves denote using just the lower diabatic PES with the results scaled by the statistical factor of 1/2, and points denote the experimental results (5). The ratio r^{34}/r^{44} for $\alpha = 0.9$ is represented by the solid and dashed curves and the solid point. The ratio r^{34}/r^{33} for $\alpha = 0.5$ is represented by the dot−dashed and dot−dot−dashed curves and the open point.

In the treatment of isotopologue association rates occurring for a particular $^3He/^4He$ mixture ratio, it is convenient to scale these rates by the expected statistical rates (i.e., the expected rates assuming all rate coefficients are unity). Under the assumption of no exchange, the scaled association rates are given by

$$r^{33} = \frac{d[^3He_2^+]'}{dt} = \frac{(1-\alpha)k_{eff}^{333} + \alpha k_{eff}^{334}}{1+\alpha(K_{eq}-1)} \quad (15)$$

$$r^{34} = \frac{d[(^3He^4He)^+]'}{dt} = \frac{(1-\alpha)(k_{eff}^{343} + K_{eq}k_{eff}^{433}) + \alpha(k_{eff}^{344} + K_{eq}k_{eff}^{434})}{2(1+\alpha(K_{eq}-1))} \quad (16)$$

$$r^{44} = \frac{d[^4He_2^+]'}{dt} = \frac{((1-\alpha)k_{eff}^{443} + \alpha k_{eff}^{444})K_{eq}}{1+\alpha(K_{eq}-1)} \quad (17)$$

where the prime denotes a scaled value, α is the fraction of ^4He in the mixture, and K_{eq} is the equilibrium constant for reaction 14 [$K_{eq} = \exp(-7.32\ cm^{-1}/k_BT)$], which is included because reaction 14 is very much faster than three-body association under typical experimental conditions, causing the $[^3He^+]$ and $[^4He^+]$ concentrations to deviate from their statistical expectation. The ratios, r^{34}/r^{44} and r^{34}/r^{33}, as given by eqs 15−17, are plotted as a function of T in Figure 5a, for α values of 0.5 and 0.9 with k_{eff} values determined using the two PESs including coupling and also using just the lower diabatic PES with the results scaled by the statistical factor of 1/2. Comparing these two approaches clearly demonstrates a type 2 SIKIE enhancement factor of approximately 2.25 near room temperature, with the effect increasing with decreasing temperature.

The values of α were chosen because they are close to those used in the experimental study; however, a direct comparison of the theoretical and experimental results requires some consideration of the experimental methodology. In the experiment, values for r^{34}/r^{44} and r^{34}/r^{33} were determined mass spectrometrically by taking the appropriate ratios of $^3He_2^+$, $(^3He^4He)^+$, and $^4He_2^+$ product ion intensities as a function of helium inlet pressure into the ion source. With increasing helium pressure in the ion source, isotope exchange reactions like

$$^3He_2^+ + {}^4He \rightleftarrows (^3He^4He)^+ + {}^3He \quad (18)$$

become increasingly important and, ultimately, will bring the isotopic composition of the helium dimer ion to an equilibrium distribution. Thus, the nascent kinetic isotope effects were experimentally estimated by a linear extrapolation of the low-pressure measurements to zero pressure. This process resulted in estimates of $r^{34}/r^{44} = 3.07 \pm 0.02$ for $\alpha = 0.912$ and $r^{34}/r^{33} = 2.88 \pm 0.06$ for $\alpha = 0.48$. Although the experimental study reported that these measurements were made at room temperature, a review of the experimental conditions revealed that this is not correct. Prior to entering the ion source, the helium was cooled to liquid nitrogen temperature; however, within the ion source, the helium was warmed because the ionizing electrons were produced from a hot rhenium filament. Thus, the helium was unlikely to be in thermal equilibrium, and furthermore, the temperature gradients would be pressure dependent. Nevertheless, subsequent work with this ion source suggests that a temperature of 120 ± 20 K is a fair estimation of the temperature conditions under which the data were taken.

Comparing the experimental and theoretical results in Figure 5a and considering that the experimental results necessarily demonstrate the combined consequences of all KIEs, the present results strongly support the experimental conclusions[5] of a type 2 SIKIE operating in the forward direction of reaction 1. Complete experimental−theoretical agreement is not expected without a detailed treatment of reaction 2 because, as noted in the justification of the uniform β_L approximation, this parameter can be expected to demonstrate a dependence on the isotopic composition of the energized complex.

It is also interesting to consider statistical atom exchange as an alternative assumption for describing the energy transfer dynamics of reaction 2. Under this assumption, the scaled formation rates are given by

$$r^{33} = \frac{d[^3He_2^+]'}{dt} = \frac{(1-\alpha)k_{eff}^{333} + \alpha(k_{eff}^{334} + k_{eff}^{343} + K_{eq}k_{eff}^{433})/3}{1+\alpha(K_{eq}-1)} \quad (19)$$

$$r^{34} = \frac{d[(^3He^4He)^+]'}{dt} = \frac{(1-\alpha)(k_{eff}^{334} + k_{eff}^{343} + K_{eq}k_{eff}^{433}) + \alpha(k_{eff}^{344} + K_{eq}(k_{eff}^{434} + k_{eff}^{443}))}{3(1+\alpha(K_{eq}-1))} \quad (20)$$

$$r^{44} = \frac{d[^4He_2^+]'}{dt} = \frac{(1-\alpha)(k_{eff}^{344} + K_{eq}k_{eff}^{434} + K_{eq}k_{eff}^{443})/3 + \alpha K_{eq}k_{eff}^{444}}{1+\alpha(K_{eq}-1)} \quad (21)$$

The ratios r^{34}/r^{44} and r^{34}/r^{33} as given by eqs 19−21 are plotted as a function of T in Figure 5b for α values of 0.5 and 0.9, with k_{eff} values again determined using the two PESs including coupling and also using just the lower diabatic PES with the results scaled by the statistical factor of 1/2. A comparison of

Figure 5a and b shows that, as expected, the assumption of statistical exchange for reaction 2 erodes but does not eliminate the effect of type 2 SIKIE in reaction 1. Furthermore, the comparison strongly supports the experimental conclusion[5] that the energy transfer stabilization step proceeds largely without atom exchange.

Finally, although this work and all experimental work on He_2^+ formation have focused on low pressure conditions, it is interesting to consider the consequences of high pressure conditions on possible SIKIEs even though the increased importance of isotope exchange reactions would be an experimental complication that might not be easily addressed. Theoretically, the present framework would have to be modified to also include an explicit consideration of the direct three-body recombination mechanism

$$He^+ + 2He \rightarrow He_2^+ + He \qquad (22)$$

Because the reactants in this mechanism experience a 3-fold BO degeneracy, whereas the products are nondegenerate, it is conceivable that reaction 22 could demonstrate type 2 SIKIEs. A full consideration of this question would involve the determination of the three relevant BO PESs and the isotopic-dependent coupling between them. Such a consideration is beyond the scope of this study. In the context of high pressure (perhaps, combined with low temperature), it can be noted that a chaperone formation mechanism

$$He_2 + He^+ \rightarrow He_2^+ + He \qquad (23)$$

may become important. Considering that the neutral helium dimer potential supports a bound state for only the $^4He_2$ isotopologue, reaction 23 would be expected to demonstrate an unusual KIE, but not one that has nuclear symmetry origins. However, if the consequences of reactions 22 and 23 are neglected, and the high pressure limit is defined simply as $w \gg k_i$, then eq 3 makes clear that type 2 SIKIE would be expected to be preserved under these conditions for He_2^+ formation.

Conclusion

Type 2 SIKIE in the three-body formation of He_2^+ has been clearly established in a first-principles theoretical treatment. In large measure, the phenomenon proceeds very much as anticipated in the earlier experimental study, for temperatures in the 100−400 K range. In the low-temperature regime, however, type 2 SIKIE is very much determined by the properties of individual resonance states; indeed, the very dramatic role played by Feshbach resonances at very low temperatures was not anticipated because, at the time of the experimental study, it was not known that the upper potential supported bound levels. These results demonstrate that the common practice of applying a simple statistical weighting factor to account for the dynamical effects of asymptotically degenerate adiabatic potential surfaces should be utilized with increased care.

Although the present demonstration focuses on a relatively simple atomic collision, there is no reason to believe that analogues of this process are not operating in the more complex ion−molecule association reactions, where this effect has been inferred.[4,6,7] In addition, this phenomenon had been suggested previously[33] as playing a role in the very unusual KIEs observed for the three-body association of ozone, with recent calculations[34−35] suggesting possible contributory effects from nonadiabatic coupling of various PESs in the $O + O_2$ entrance channel. Although recent experimental results[36] have shown that the observed KIEs cannot be dominantly controlled by type 2 SIKIEs, as they are for He_2^+ association, there is, nevertheless, no reason to believe that they do not have a contributory influence, which may combine with other suggested mechanisms[10−14,37−40] to produce the overall effect.

Acknowledgment. Grateful acknowledgment is made to the Robert A. Welch Foundation (D-1293 and D-1523) for support of this work. Acknowledgment is also made to the office of Advanced Scientific Computing Research, Mathematical, Information, and Computational Sciences Division of the U.S. Department of Energy under Contract No. DE-FG03-02ER25534. We would also like to thank a referee for a very detailed and helpful review.

JA0517419

(33) Gellene, G. I. *Science* **1996**, *274*, 1344.
(34) Rosmus P.; Palmieri, P.; Schinke, R. *J. Chem. Phys.* **2002**, *117*, 4871.
(35) Tashiro M.; Schinke, R. *J. Chem. Phys.* **2003**, *119*, 10186.
(36) Mauersberger, K.; Erbacher, B.; Krankowsky, D.; Günther, J.; Nickel, R. *Science* **1999**, *283*, 370.
(37) Babikov, D; Kendrick, B. K.; Walker, R. B.; Schinke, R.; Pack, R. T. *Chem. Phys. Lett.* **2003**, *372*, 686.
(38) Babikov, D.; Kendrick, B. K.; Walker, R. B.; Pack, R. T.; Fleurat-Lesard, P.; Schinke, R. *J. Chem. Phys.* **2003**, *119*, 2577.
(39) Charlo, D.; Clary, D. C. *J. Chem. Phys.* **2002**, *117*, 1660.
(40) Charlo, D.; Clary, D. C. *J. Chem. Phys.* **2004**, *120*, 2700.